Near-Capacity Turbo Coded Soft-decision Aided DAPSK/Star-QAM

Dandan Liang, *Student Member, IEEE*, Soon Xin Ng, *Senior Member, IEEE*, and Lajos Hanzo, *Fellow, IEEE*

University of Southampton
Communications Research Group
Southampton, SO17 1BJ, U.K.
E-Mail: {dl4e08,sxn,lh}@ecs.soton.ac.uk

Abstract— Low-complexity non-coherently detected Differential Amplitude and Phase-Shift Keying (DAPSK) schemes constitute an ideal candidate for wireless communications. In this paper, we derive the soft-output probability formulas required for the soft-decision based demodulation of DAPSK, which are then invoked for Turbo Coded (TC) transmissions. Furthermore, the achievable throughput characteristics of the family of M-ary DAPSK schemes are provided. It is shown that the proposed 4-ring based TC assisted 64-ary DAPSK scheme achieves a coding gain of about 4.2 dBs in comparison to the identical-throughput TC assisted 64-ary Differential Phase-Shift Keying (64-DPSK) scheme at a bit error ratio of 10^{-5}.

Index Terms— Soft-decision, Iterative detection, DAPSK, TC, Correlated Rayleigh fading channel, Near-capacity transceivers

I. INTRODUCTION

Coherent detection aided square-constellation based Quadrature Amplitude Modulation (QAM) requires accurate Channel State Information (CSI) in order to avoid false phase-locking of the carrier-recovery scheme, especially when communicating over Rayleigh fading channels [1]–[5]. As a remedy, Differential Amplitude and Phase-Shift Keying (DAPSK) was conceived for dispensing with CSI, albeit naturally at the cost of a performance loss. This scheme was termed as Star-QAM in [6]. Non-coherent schemes are particularly beneficial in cooperative communications, where it is unrealistic to estimate all mobile-to-mobile channels [7], [8]. Let us define the notation M-DAPSK (M_a,M_p) representing M_a amplitudes and M_p different phases, which may also be denoted as M_a-DASK/M_p-DPSK or Star-QAM. The authors of [9], [10] have further improved the performance of M-DAPSK (M_a,M_p) schemes. However, despite its attractive performance versus complexity characteristics, surprisingly soft-decision based demodulation has not been conceived for these M-DAPSK (M_a,M_p) schemes. This also implies that without soft-decision based demodulation, the full potential of sophisticated channel coding or coded modulation schemes cannot be entirely exploited. Hence, when channel coding is incorporated into

M-DAPSK (M_a,M_p) as in [6], its performance is far from the channel capacity due to the employment of hard-decision based demodulation. The twin-ring based soft-decision assisted Star-QAM scheme was proposed for Iteratively Detected Bit-Interleaved Coded Modulation (BICM-ID) in [11]. As a further improvement, in this contribution Turbo Coding (TC) [12] is employed because its Extrinsic Information Transfer (EXIT) curve shape was found to have a better match with that of the M-DAPSK (M_a,M_p) demapper. Which is beneficial, because the smaller the area between these two EXIT curves, the closer this scheme operates to the achievable capacity [8], [14]. Our novel contributions are:

- we will first solve the open problem of deriving the soft-decision demodulation probability formulas for M-DAPSK (M_a,M_p) schemes, which have more than two concentric PSK constellations;
- Secondly, the performance benefits of using the new formulas will be quantified in the context of TC schemes invoked for communications over correlated Rayleigh fading channels at a normalised Doppler frequency of 0.01;
- Finally, the channel capacity of M-DAPSK (M_a,M_p) will be quantified for the the sake of demonstrating that our proposed scheme constitutes a near-capacity design.

This paper is organised as follows. In Section II, the soft-decision demodulation of M-DAPSK (M_a,M_p) aided TC will be presented. Our results will be discussed in Section III and our conclusions are offered in Section IV.

II. SYSTEM MODEL AND ANALYSIS

Fig. 1 shows the simplified schematic of the near-capacity TC aided M-DAPSK (M_a,M_p) scheme, where the number of constellation points is $M = M_a * M_p = 2^m$, while the number of amplitudes is $M_a = 2^{m_a}$ and the number of phases per amplitude circle is $M_p = 2^{m_p}$. More explicitly, m, m_a and m_p denotes the total number of modulated bits/symbol, the number of bits assigned to the amplitude rings and that assigned select the phases, respectively. A sequence of information symbols is encoded by a rate-1/2 TC encoder for generating a sequence of coded symbols. Out of the total of m bits, m_a bits will be used for selecting
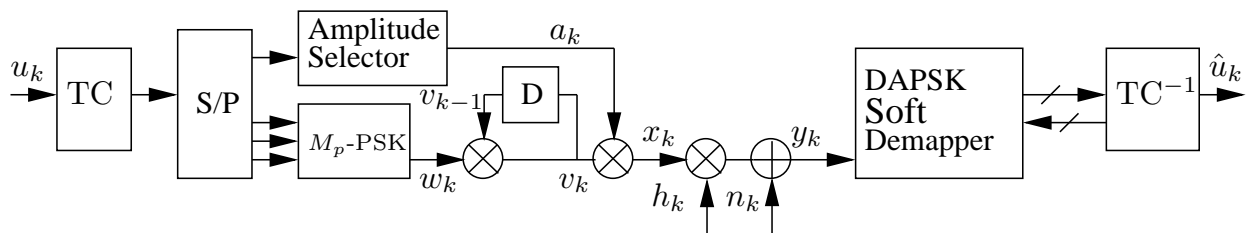
Fig. 1: The schematic of the M-DPSK (M_a,M_p) aided TC scheme, where the interleavers and de-interleavers between the encoder/decoder and mapper/de-mapper are not shown for simplicity.

the amplitude of the Phase-Shift-Keying (PSK) ring, while the remaining (m − m_a) bits will be used for selecting the phase of the complex-valued M-DPASK (M_a,M_p) symbol x_k, where the subscript k denotes the symbol index. As shown in Fig. 1, the TC-encoded M-DPASK symbol is corrupted by both the complex-valued Rayleigh fading channel coefficient h_k and the Additive White Gaussian Noise (AWGN) n_k, when it is transmitted to the receiver. Iterative detection is then carried out by exchanging extrinsic information between the M-DAPSK soft demapper and TC decoder based on the received sequence $\{y_k\}$ without exploiting any CSI.

A. M-DAPSK Mapper

As seen in Fig. 1, the M-DAPSK (M_a,M_p) mapper consists of three components, namely the amplitude selector, the M_p-PSK mapper and a differential encoder. The M_p-PSK mapper and the differential encoder jointly form a conventional M_p-level DPSK (M_p-DPSK) mapper. The m_a bits of the TC-encoded symbol are used for selecting one of the M_a possible amplitude circles. The remaining (m − m_a) bits are used by the M_p-DPSK mapper. Note that similar to any DPSK scheme, we insert a reference symbol at the beginning of each differentially encoded transmission frame before the M-DAPSK (M_a,M_p) mapper. We use the 64-DAPSK (4,16) scheme as an example for illustrating the philosophy of our proposed soft-decision based demapper.

1) Amplitude Selection: $m_a = 2$ bits are used for selecting the amplitude of the PSK ring, a_k. The four possible amplitude values are denoted as $a^{(1)}$, $a^{(2)}$, $a^{(3)}$ and $a^{(4)}$, respectively. Table I illustrates the procedure of amplitude selection. Note that the classic Set Partitioning (SP) [13] method is employed in the mapper. This amplitude selection mechanism may be

a_k		m_a-bits (b_5 and b_4)			
		00	01	10	11
a_{k-1}	$a^{(1)}$	$a^{(1)}$	$a^{(2)}$	$a^{(3)}$	$a^{(4)}$
	$a^{(2)}$	$a^{(2)}$	$a^{(3)}$	$a^{(4)}$	$a^{(1)}$
	$a^{(3)}$	$a^{(3)}$	$a^{(4)}$	$a^{(1)}$	$a^{(2)}$
	$a^{(4)}$	$a^{(4)}$	$a^{(1)}$	$a^{(2)}$	$a^{(3)}$

TABLE I: Table to generate the amplitude a_k.

referred to as M_a-level Differential Amplitude Shift Keying (M_a-DASK). After normalisation to a symbol energy of unity, we have $a^{(1)} = 1/\sqrt{3.58}$, $a^{(2)} = 1.4/\sqrt{3.58}$, $a^{(3)} = (1.4)^2/\sqrt{3.58}$ and $a^{(4)} = (1.4)^3/\sqrt{3.58}$. The amplitude value of the reference symbol is given by $a_0 = a^{(1)}$. Fig. 2 shows

the constellation diagrams of 8-DAPSK (4,2), 16-DAPSK (4,4), 32-DAPSK (4,8) and 64-DAPSK (4,16).
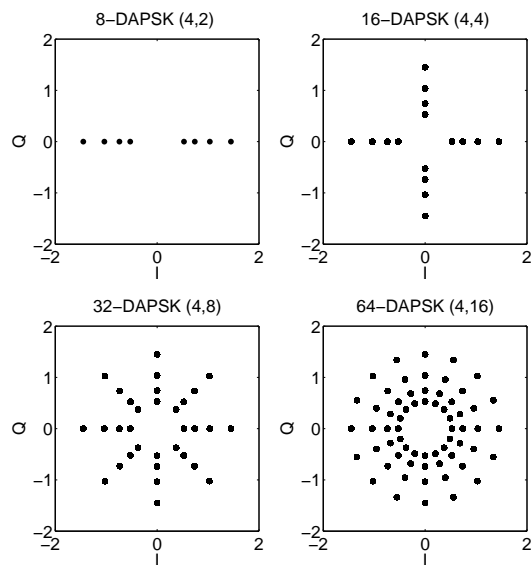
Fig. 2: Constellation diagrams of the M-DAPSK (4, M_p) modulation schemes.

2) Phase Selection: When we consider $m_p = 4$, the kth differentially encoded symbol v_k can be expressed as:

$$v_k = v_{k-1}w_k, \tag{1}$$

where $x_k = \mu(b_3\ b_2\ b_1\ b_0)$ is the kth 16-PSK symbol based on the 16-PSK mapping function of $\mu(.)$, while v_{k-1} is the $(k-1)$st 16-DPSK symbol and $|v_k|^2 = 1$. The reference symbol of the 16-DPSK part of the constellation is given by $v_0 = \mu(0\ 0\ 0\ 0)$.

The kth 64-DAPSK symbol is then given by:

$$x_k = a_k v_k, \tag{2}$$

where we have $a_k \in \{a^{(1)}, a^{(2)}, a^{(3)}, a^{(4)}\}$.

B. M-DAPSK Soft Demapper

As in all transceivers, the soft-decision based M-DAPSK (M_a,M_p) block is placed before the TC decoder, as shown in Fig. 1. The kth received symbol may then be written as:

$$y_k = h_k x_k + n_k = h_k a_k v_k + n_k \ , \tag{3}$$

where h_k is the Rayleigh fading channel's coefficient, while n_k represents the AWGN having a variance of $N_0/2$ per dimension. Assuming a slowly Rayleigh fading channel, where we have $h_k \approx h_{k-1}$, we can rewrite (3) using (1) as:

$$
\begin{aligned}
y_k &= h_{k-1} a_k v_{k-1} w_k + n_k \ , \\
&= \frac{a_k}{a_{k-1}} \left(y_{k-1} - n_{k-1} \right) w_k + n_k \ , \\
&= p_k y_{k-1} w_k + \tilde{n}_k \ ,
\end{aligned}
\tag{4}
$$

where $p_k = \frac{a_k}{a_{k-1}}$ is the ratio of the kth and $(k-1)$st amplitudes, while $\tilde{n}_k = -\frac{a_k}{a_{k-1}} n_{k-1} w_k + n_k$ is the effective noise.

1) Amplitude Detection: $(2 \cdot M_a - 1)$ amplitude ratios can be derived from the M_a-PSK ring amplitudes of M-DAPSK (M_a, M_p). It may be readily shown that for 64-DAPSK (4,16), we have:

$$
p_k =
\begin{cases}
R_{-3} &= a^{(1)}/a^{(4)} \\
R_{-2} &= a^{(1)}/a^{(3)} = a^{(2)}/a^{(4)} \\
R_{-1} &= a^{(1)}/a^{(2)} = a^{(2)}/a^{(3)} = a^{(3)}/a^{(4)} \\
R_{0} &= a^{(1)}/a^{(1)} = a^{(2)}/a^{(2)} \\
&= a^{(3)}/a^{(3)} = a^{(4)}/a^{(4)} \\
R_{1} &= a^{(2)}/a^{(1)} = a^{(3)}/a^{(2)} = a^{(4)}/a^{(3)} \\
R_{2} &= a^{(3)}/a^{(1)} = a^{(4)}/a^{(2)} \\
R_{3} &= a^{(4)}/a^{(1)} \ .
\end{cases}
\tag{5}
$$

When the noise power is low, the amplitude ratio p_k may be approximated as:

$$
\begin{aligned}
\frac{|y_k|}{|y_{k-1}|} &= \frac{|h_k a_k v_k + n_k|}{|h_{k-1} a_{k-1} v_{k-1} + n_{k-1}|} \ , \tag{6} \\
&\approx \frac{|a_k|}{|a_{k-1}|} \ , \\
&\approx p_k \ . \tag{7}
\end{aligned}
$$

2) Probability Computation: The effective noise variance of $\tilde{n}_k$ in (4) depends on the amplitude ratio used at time instant k, which can be computed as:

$$
\widetilde{N}_0 = N_0 + |p_k|^2 |w_k|^2 N_0 = N_0(1 + |p_k|^2) \ , \tag{8}
$$

where $\widetilde{N}_0 = (1 + R_q^2) N_0 = N_0^{(q)}$, $q \in \{-3, -2, -1, 0, 1, 2, 1, 3\}$. Based on (4) we can express the probability of receiving y_k conditioned on the transmission of b_0, b_1, b_2, b_3, b_4 and b_5 as in (9). The bit-probabilities can then be then can be converted to the Log-Likelihood Ratio (LLR) [14] based representations of b_i, $i \in \{0, 1, 2, 3, 4, 5\}$ where we have $w^{(m)} = \mu(b_3 b_2 b_1 b_0)$ and μ is the conventional 16-PSK mapper function.

$$
\begin{aligned}
P(y_k | w^{(m)}, b_5 b_4 = 00) &= \frac{1}{\pi N_0^{(0)}} e^{\frac{-\left|y_k - y_{k-1} R_0 w^{(m)}\right|^2}{N_0^{(0)}}} \ , \\[2ex]
P(y_k | w^{(m)}, b_5 b_4 = 01) &= \frac{1}{\pi N_0^{(1)}} e^{\frac{-\left|y_k - y_{k-1} R_1 w^{(m)}\right|^2}{N_0^{(1)}}} \\
&+ \frac{1}{\pi N_0^{(-3)}} e^{\frac{-\left|y_k - y_{k-1} R_{-3} w^{(m)}\right|^2}{N_0^{(-3)}}} \ , \\[2ex]
P(y_k | w^{(m)}, b_5 b_4 = 10) &= \frac{1}{\pi N_0^{(2)}} e^{\frac{-\left|y_k - y_{k-1} R_2 w^{(m)}\right|^2}{N_0^{(2)}}} \\
&+ \frac{1}{\pi N_0^{(-2)}} e^{\frac{-\left|y_k - y_{k-1} R_{-2} w^{(m)}\right|^2}{N_0^{(-2)}}} \ , \\[2ex]
P(y_k | w^{(m)}, b_5 b_4 = 11) &= \frac{1}{\pi N_0^{(3)}} e^{\frac{-\left|y_k - y_{k-1} R_3 w^{(m)}\right|^2}{N_0^{(3)}}} \\
&+ \frac{1}{\pi N_0^{(-1)}} e^{\frac{-\left|y_k - y_{k-1} R_{-1} w^{(m)}\right|^2}{N_0^{(-1)}}}
\end{aligned}
\tag{9}
$$

III. SIMULATION RESULTS

Computer simulations have been performed for characterising the proposed soft-decision based M-DAPSK $(4, M_p)$ demodulation technique in the context of TC coding schemes. In order to benchmark our proposed method, the classic square-constellation 64-QAM and 64-DPSK schemes were employed. The simulation parameters are shown in Table II.

Modulation	64-DAPSK(4,16), 32-DAPSK(4,8), 16-DAPSK(4,4) 8-DAPSK(4,2), 64-QAM, 64-DPSK
Mapping	Set Partitioning (SP)
Coding	TC
Constituent Code	Half-rate Recursive Systematic Convolutional (RSC) code Code Polynomial G=[15 17]
Code Memory	3
Outer iterations	4
Inner TC iterations	2
Decoder	Approximate Log-MAP
Symbols per 64-DAPSK block	400, 4000
Number of 64-DAPSK blocks per TC block	1, 10
Number of TC blocks	5000
Channel	Correlated Rayleigh fading channel having a normalised Doppler frequency of 0.01

TABLE II: System parameters.

Firstly, the EXIT Charts of the proposed system is presented for analysing the 64-DAPSK (4,16) scheme. Fig. 3 illustrates
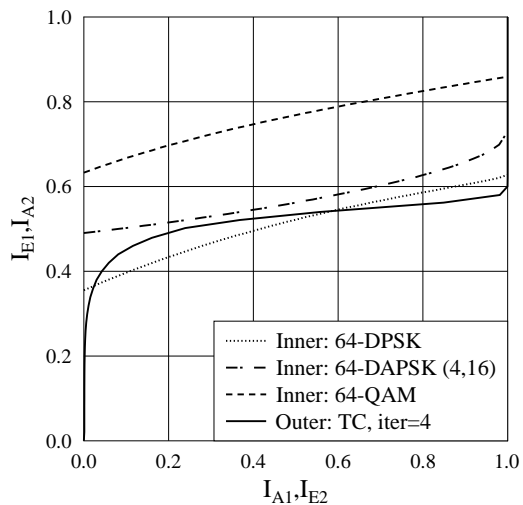
Fig. 3: EXIT Charts of the 64-QAM, 64-DAPSK (4,16) and 64-DPSK aided TC schemes when communicating over a correlated Rayleigh channel at SNR=17.5 dB. The SNR-independent EXIT curve of the outer TC decoder is also shown. The corresponding simulation parameters are presented in Table. II

three inner decoder [1] EXIT curves, namely those of the 64-QAM, 64-DAPSK (4,16) and 64-DPSK schemes, together with the EXIT curve of the outer TC decoder. It is worth noting that the area under the EXIT curve of the inner decoder is approximately equal to the channel capacity [7], [15], [16]. It is then clear from Fig. 3 that the area under the square-constellation 64-QAM scheme's EXIT curve is larger than that under the 64-DAPSK (4,16) scheme's curve, which is in turn higher than that of the 64-DPSK arrangement. It was also demonstrated in [7], [8] that an open EXIT chart tunnel implies having an infinitesimally low BER. Hence we may argue based on Fig. 3 that a vanishingly low BER may be achieved by the TC aided 64-DAPSK (4,16) scheme for SNR values in excess of 17.5 dB. By contrast, no open EXIT chart tunnel is maintained for the same SNR value in the case of the 64-DPSK benchmark scheme.

The corresponding BER versus SNR performance is depicted in Fig. 4, which compares the performance of the 64-QAM, 64-DAPSK (4,16) and 64-DPSK aided TC schemes, when communicating over correlated Rayleigh fading channels using different transmission block lengths and turbo-interleaved block lengths. More explicitly, as seen in Table II, each block consists of 400 or 4000 modulated symbols. The TC block length is given by the number of modulated symbols per 64-DAPSK transmission block times the number of transmission blocks per TC block. When the number of 64-DAPSK modulated transmission blocks per TC block is one, which corresponds to the curve marked by circles in Fig. 4, the SNR difference between the classic coherently detected

---

[1]In serially concatenated and turbo-detected schemes the soft-output demodulator is often referred to as the inner terminology decoder, for the sake of a unified.
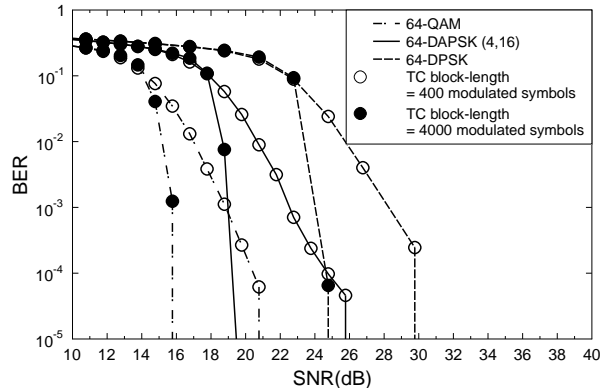
Fig. 4: BER versus SNR(dB) performance comparison of the 64-QAM, 64-DAPSK (4,16) and 64-QAM schemes for transmission over correlated Rayleigh fading channels. The corresponding system parameters are summarized in Table. II. A TC block-length of 400 modulated symbols corresponds to one 64-DAPSK block-length, while a 4000-modulated-symbol TC block corresponds to ten 64-DAPSK block-length.
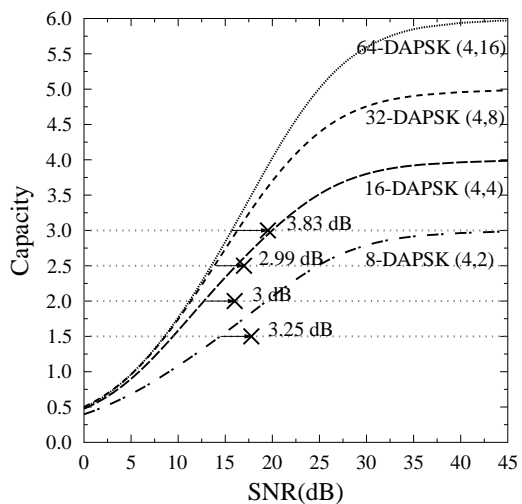
Fig. 5: Achievable throughput versus SNR for with the systems of Fig. 2 for transmission over correlated Rayleigh fading channels, while using TC block length of 4000 modulated symbols.

square-constellation 64-QAM and our low-complexity 64-DAPSK dispensing with power-thirsty channel-estimation is 5 dB. As a substantial further benefit, our scheme outperforms 64-DPSK by about 4.2 dB. When the number of 64-DAPSK blocks per TC block is increased to ten (the curve marked by filled circles), all the BER performances are improved, but the SNR differences remain similar. In general, the longer the TC block-length, the better the BER performance becomes gradually approaching channel capacity.

Finally, the achievable throughput of the M-DAPSK (4, M_p) modem family is characterised in Fig. 5, where the curves were generated by evaluating the area under the

corresponding EXIT curves, as detailed in [8], [14]. The large crosses represent the SNR required for the corresponding modulation schemes to achieve an identical throughput to each other at a target BER of 10^{-5}. The horizontal grey dotted lines represent the throughput values of the different modulation schemes considered. For example, 1.5 is that of TC aided 8-DAPSK (4,2). Fig. 5 also shows the SNR discrepancy between the various schemes and the corresponding channel capacity. More specifically, the TC aided 64-DAPSK (4,16) scheme is capable of reliably operating approximately 3.83 dB away from its capacity, while the TC aided 32-DAPSK (4,8) arrangement operates approximately 2.99 dB away from its capacity.

IV. Conclusions

The symbol-to-bit soft-demapper probability formulas of the 64-DAPSK (4,16) scheme were derived and its soft-decision aided performance was investigated in the context of a TC scheme. The 64-DAPSK-TC scheme outperforms the identical-throughput 64-DPSK-TC scheme by about 4.2 dB at a BER of 10^{-5}, when communicating over correlated Rayleigh fading channels having a normalised Doppler frequency of 0.01. Finally, the achievable throughput characteristics of the M-DAPSK $(4,M_p)$ modem-family were presented. Our future research will improve the resilience of these schemes against high Doppler frequencies with the aid of multiple-symbol differential detection (MSDD) [8]. We will also conceive low-complexity MSDD schemes with the aid of sphere decoding [8].

References

[1] E. Issman and W. Webb, "Carrier recovery for 16-level QAM in mobile radio," *IEE colloquium on multi-level modulation*, pp. 9/1 – 9/8, March 1990.

[2] L. Hanzo, S. X. Ng, T. Keller, and W. Webb, *Quadrature Amplitude Modulation: From Basics to Adaptive Trellis-Coded, Turbo-Equalised and Space-Time Coded OFDM, CDMA and MC-CDMA Systems Digital Communications*, 2nd ed. Wiley-IEEE Press, 2004.

[3] L. Chen, H. Kusaka, and M. Kominami, "Blind phase recovery in QAM communication systems using higher order statistics," *Signal Processing Letters, IEEE*, vol. 3, no. 5, pp. 147 –149, may. 1996.

[4] Y. Wang and E. Serpedin, "A class of blind phase recovery techniques for higher order QAM modulations: estimators and bounds," *Signal Processing Letters, IEEE*, vol. 9, no. 10, pp. 301 – 304, oct. 2002.

[5] H. Rohling and V. Engels, "Differential amplitude phase shift keying (dapsk)-a new modulation method for dtvb," in *Broadcasting Convention, 1995. IBC 95., International*, Sept. 1995, pp. 102 –108.

[6] W. Webb, L. Hanzo, and R. Steele, "Bandwidth-efficient QAM schemes for Rayleigh-fading channels," *IEE Proceedings*, vol. 138, no. 3, pp. 169–175, June 1991.

[7] L. Hanzo and O. Alamri and N. El-Hajjar and N. Wu, *Near-Capacity Multi Functional MIMO Systems*. John Wiley & Sons, Ltd, May 2009.

[8] L. Hanzo, Y. Akhtman, L. Wang, M. Jiang, *MIMO-OFDM for LTE, WiFi and WiMAX: Coherent versus Non-coherent and Cooperative Turbo Transceivers*. John Wiley & Sons, Ltd, October 2010.

[9] C.-D. Chung, "Differentially amplitude and phase-encoded QAM for the correlated Rayleigh-fading channel with diversity reception," *IEEE Transactions on Communications*, vol. 45, no. 3, pp. 309 – 321, March 1997.

[10] Y. Ma, Q. T. Zhang, R. Schober and S. Pasupathy, "Diversity reception of DAPSK over generalized fading channels," *IEEE Transactions on Wireless Communications*, vol. 4, no. 4, pp. 1834 – 1846, July 2005.

[11] D. Liang, S. X. Ng, and L. Hanzo, "Soft-decision Star-QAM aided BICM-ID," *Signal Processing Letters, IEEE*, vol. 18, no. 3, pp. 169 –172, 2011.

[12] C. Berrou and A. Glavieux and P. Thitimajshima, "Near Shannon limit error-correcting coding and decoding: Turbo codes," in *Proceedings of the International Conference on Communications*, Geneva, Switzerland, May 1993, pp. 1064–1070.

[13] M. Rohling, T. May, K. Bruninghaus, and R. Grunheid, "Broad-band OFDM radio transmission for multimedia applications," *Proceedings of the IEEE*, vol. 87, no. 10, pp. 1778 –1789, Oct. 1999.

[14] L. Hanzo, T. H. Liew, B. L. Yeap, R. Y. S. Tee, S. X. Ng, *Turbo Coding, Turbo Equalisation and Space-Time Coding: EXIT-Chart-Aided Near-Capacity Designs for Wireless Channels, 2nd Edition*. Wiley-IEEE Press, 2011.

[15] S. ten Brink, "Convergence behaviour of iteratively decoded parallel concatenated codes," *IEEE Transactions on Communications*, vol. 49, no. 10, pp. 1727–1737, October 2001.

[16] J. Kliewer, S. X. Ng, and L. Hanzo, "Efficient computation of EXIT functions for non-binary iterative decoding," *IEEE Transactions on Communications*, vol. 54, no. 12, pp. 2133–2136, December 2006.